JOURNAL OF MATERIALS SCIENCE 31 (1996) 1809–1814

Liquid self-diffusion in pores of hardened gypsum: pulsed field gradient NMR study

A. V. FILIPPOV, E. V. KHOSINA, V. G. KHOSIN
Kazan Civil Engineering Institute, Zelenaya Str. 1, Kazan, 420043 Tatarstan, Russia

The self-diffusion of liquid confined in pores of gypsum was studied using NMR method with pulsed magnetic field gradient at 30 °C. The starting weight ratios of water to gypsum were equal to 0.4, 0.5, 0.6, 0.8 and 1. The hardening process occurred at 23 °C. The pores of gypsum form a permeable system. This fact allows us to use two liquids with the diffusion coefficients differing by a factor of 100 such as water and polypropyleneoxide with $M = 1025$. Thus, the length scale of the study was broadened to 2.5×10^{-7}–4.2×10^{-5} m. Dependencies of echo-attenuation shape and of diffusion coefficient versus diffusion time were investigated. The slopes of echo-attenuations and values of diffusion coefficients determined for the same length scale are different for the systems with starting ratios of water to gypsum 0.4–0.6 and 0.8–1. The experimental results for the samples with lower water to gypsum ratios were interpreted in terms of a model with two levels of organization of the porous structure. The first level comprises the interconnected layers with all possible orientations. The second level comprises the barriers distributed inside the layers. Diffusion of the liquid molecules inside the layer is restricted due to collisions with the barriers. In the samples with greater water-to-gypsum starting ratios, pores larger than 50 μm were discovered. The width of layer, the barrier separation and the minimum of the layer stretching were estimated.

1. Introduction

Many physical properties of porous solids depend on the pore surface and structural development [1], and thus these are subjects of considerable relevance for many researchers. One of the porous materials of both applied and fundamental interest is hardened gypsum [2–4].

The hardening process of gypsum involves several stages [2], with formation of gypsum dihydrate being the most important for structural development:

$$CaSO_4 \cdot 0.5H_2O + 1.5H_2O \rightarrow CaSO_4 \cdot 2H_2O$$

with further crystallizing from the saturated solution during 20–40 min. An essential condition for the hydration reaction to be completed is a significant abundance of water (approximately four times as much as is necessary for the reaction). So the resulting product is distinguished by the increased specific porosity (up to 40–60%) [2, 3].

Since crystallization occurs at conditions far from thermodynamic equilibrium, the structure formed differs from a perfect crystal to a great extent. It represents an agglomerate of intergrowing crystallites. The structure of such an agglomerate may be described in terms of a fractal approach similar to other porous systems [5, 6].

Water confined in the intercrystalline space is a bad solvent for the gypsum dihydrate (about 2 g per litre in terms of $CaSO_4$), so the gypsum structure does not change after water evaporation and the following reinjection of water (except in cases where this operation is repeated many times).

Pores of gypsum are interconnected, with the average dimensions being more than 0.05 μm corresponding to the macropores [3, 4]. About 95% of pores are capillary ones. Water in pores can be either mobile (bulk) or adsorbed on the surface. The latter being less than 1% of the porous solid mass.

The NMR method with pulsed magnetic field gradient (NMR PMFG) has proved to be one of the most suitable methods for studying molecular diffusion in heterogeneous systems [7–9]. The method allows us to probe the structure of pores accessible for liquid molecules in varying length scales.

The purpose of this work was to study the peculiarities of liquid self-diffusion and the structure of porous space of hardened gypsum using the NMR PMFG method. For this purpose a combined analysis of the dependencies of echo-attenuations and averaged diffusion coefficients upon the diffusion time was applied. Substituting water by a less mobile liquid allowed us to broaden the length scale of the study. As a result some ideas about the gypsum porous structure were proposed.

2. Experimental details

2.1. Preparation of samples

A powder of hemiwater gypsum ($CaSO_4 \cdot 0.5H_2O$) was first heated at $T = 100$ °C for an hour to remove

0022-2461 © *1996 Chapman & Hall*

moisture. Then it was blended with distilled water in the weight ratios 1 : 0.4 (N1); 1 : 0.5 (N2); 1 : 0.6 (N3); 1 : 0.8 (N4); and 1 : 1 (N5). Blends were put into both open and sealed glass tubes. The hardening process occurred at 23 °C. Measurements were begun within 60 min after blending, and were carried out during an hour at 30 °C when the hardening process completed [2–4]. The measurements were repeated a day later. In the case of the sealed glass tubes, the previously obtained data were replicated. For the open tubes the echo amplitude fell to zero in course of time. However, if the evaporated water was compensated by the addition of a new portion, the original results were replicated. Thus, the obtained results describe equally the self-diffusion of mobile water retained after hardening and the self-diffusion of water added in pores of hardened gypsum after evaporation. The reduction of the observed signal in the unsealed samples agree with the concept of opened pores in gypsum.

2.2. Pulsed field gradient spectroscopy

The base principles of the PMFG method were described previously [7–11]. The base information obtained from the NMR PMFG experiment is the mean-squared displacement of molecules along the pulsed gradient direction $\langle x^2 \rangle$. For bulk liquid of low molecular weight, $\langle x^2 \rangle$ is determined by Gaussian statistics of molecules random walk as:

$$\langle x^2 \rangle = 2Dt_d \qquad (1)$$

where $D = D_0$ is the diffusion coefficient, and t_d is the diffusion time. The diffusion attenuation of spin-echo amplitude in this case is:

$$A(g) = A(0)\exp(-kD) \qquad (2)$$

where

$$A(0) \sim \exp(-2\tau_2/T_2)\exp(-\tau_2/T_1) \qquad (3)$$

if "stimulated echo" pulse sequence is used, τ_1 and τ_2 are the intervals between first and second and the second and third radio-frequency pulses, respectively. T_1 and T_2 are the longitudinal and transverse NMR relaxation times, $k = \gamma^2\delta^2 g^2 t_d$, γ is the gyromagnetic ratio of the nucleus; g and δ are the amplitude and duration of gradient pulse, respectively. For display of echo attenuation (EA) the coordinates log[A] versus k are usually used. For the simplest cases EA comprises a straight line with the slope equal to D.

In the more complicated cases liquid can be characterized by the spectrum of diffusion coefficients. EA, in the case of discrete spectrum, is given by:

$$A(g) \sim \Sigma[P_i\exp(-2\tau_2/T_{2i})\exp(-\tau_1/T_{1i})\exp(-kD_i)] \qquad (4)$$

where the summation is performed over the different groups of protons constituting the "NMR phases", and P_i is a relative fraction of protons in the "phase".

The experimental value of the averaged diffusion coefficient $\langle D \rangle$ can be determined as a first derivative of the EA with respect to g^2:

$$\langle D \rangle = -(\gamma^2\delta^2 t_d)^{-1} \left.\frac{\partial(\ln(A(g)))}{\partial(g^2)}\right|_{g\to 0}$$

The diffusion of molecules confined in a porous medium strongly depends on the ratio of $\langle x^2 \rangle$ to the characteristic sizes of the porous medium [6–9]. The latter parameters are the obstacle spacing d (the pore size) and a correlation length ξ. ξ is determined by the length scale above which the Gaussian statistics of random walk holds true. In extreme cases $\langle D \rangle$ does not depend on t_d. When $\langle x^2 \rangle \ll d^2$, the unrestricted diffusion regime takes place: $\langle D \rangle = D_0$. For $\langle x^2 \rangle \gg \xi^2$ a percolation regime is observed. $\langle D \rangle = D_{\mathrm{perc.}}$, with $D_{\mathrm{perc.}}$ being determined by the permeability and tortuosity of the medium. If pores are closed the dependence $\langle D \rangle \sim {t_d}^{-1}$ is observed when $\langle x_2 \rangle \geqslant d^2$.

The NMR PMFG experiment was performed using the NMR spectrometer manufactured by "Magnitnyi Resonans" [10, 11] operating at frequency 60 MHz on ^{1}H. The largest value of pulsed field gradient amplitude was equal to 40 T m^{-1}. The "stimulated echo" pulse sequence was used. The error of measurement was not more than 10% even in the worst conditions.

3. Results and discussion

3.1. Experimental results

The preliminary analysis of echo-attenuations and diffusion coefficients versus diffusion time has revealed the difference in the behaviour of the samples N1–N3 on the one hand and N4, N5 on the other. Let us consider at first the data obtained for the samples N1–N3.

Fig. 1 shows EA for bulk water and for the sample N3 that is typical for samples with low initial content

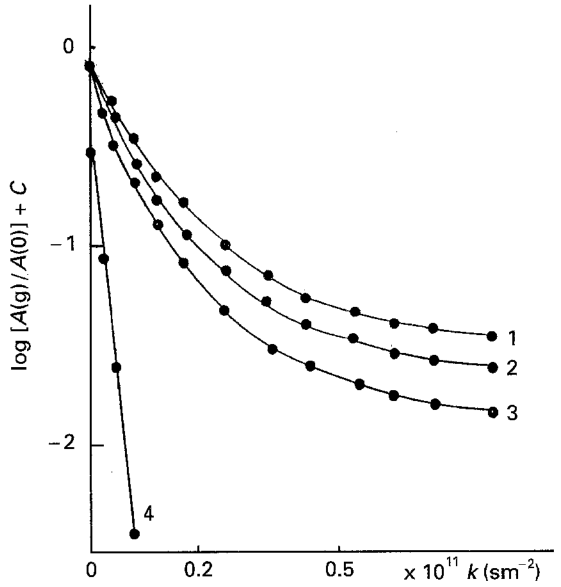

Figure 1 Echo-attenuations as the function of pulsed field gradient amplitude observed in water in bulk water (4) and in gypsum pores (sample N3) at the diffusion times t_d = 3 ms (3), 20 ms (2), 100 ms (1). C is the arbitrary constant, $k = \gamma^2\delta^2 g^2 t_d$. $\delta^2 t_d$ is a constant for all samples and all values of t_d.

of water. The echo-attenuations for water in pores (curves 1–3) are more complicated when compared to the exponential behaviour observed for bulk water (curve 4).

With t_d increases, echo-attenuations for all samples change. However, all echo-attenuations observed for samples N1–N3 can be brought in coincidence with each other if we replace the axis k by the axis k/D. Therefore, the apparent change of EA shape with t_d and water content variation is conditioned by changes of $\langle D \rangle$.

To compare the different echo-attenuations one can use an alternative to the replacement of coordinates. The use of a parameter characterizes the degree of echo-attenuation non-exponentially. We used an experimental parameter $\chi = g_{25}{}^2/2g_5^2$, where g_5 and g_{25} are the gradient amplitudes. They reduce the spin-echo amplitude by the factors 5 and 25, respectively. In the case of exponential EA, for example in bulk water, $\chi = 1$. For non-exponential EA of water confined in the pores of samples N1–N3, χ is equal to 2.2 ± 0.1.

Fig. 2 shows plots of $\langle D \rangle$ as a function of diffusion time in double logarithmic coordinates for the samples N1–N3. One can see that the values $\langle D \rangle$ are varied with water content (curves 2–4) and with diffusion time being less than the bulk water value $D_0 = 2.7 \times 10^{-9}\,\mathrm{m^2\,s^{-1}}$ (curve 1) at the same temperature.

The echo-attenuations for water in the samples N4 and N5 could be expressed as:

$$R(g) \;=\; P_1 R_1(g) + P_2 R_2(g) \qquad (4)$$

where $R(g) = A(g)/A(0)$, R_1 is the exponential component with $D = D_0$, R_2 has the same shape as EA for samples N1–N3, and $P_{1,2}$ are the relative fractions of components. P_2 increases with the increasing gypsum-to-water ratio. The observation of a component typical for bulk liquid indicates that some pores in the samples N4 and N5 have sizes larger than the maximum mean-squared displacement attainable in the experiment ($\sim 50\,\mu\mathrm{m}$).

For the systems under consideration there are no components of EA where the relation $\langle D \rangle \sim t_d^{-1}$ holds up, thus closed pores are absent.

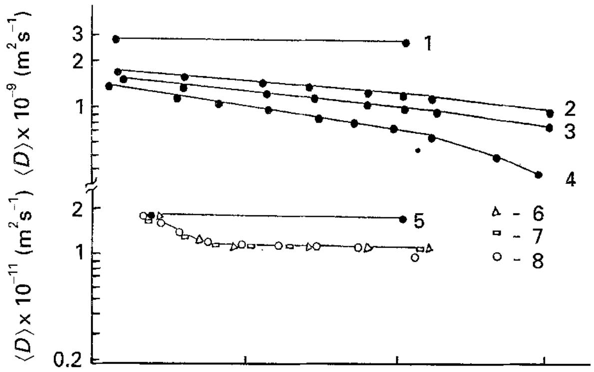

Figure 2 Plot of the averaged diffusion coefficient $\langle D \rangle$ versus t_d for water in bulk (1), and in samples N1 (4), N2 (3), N3 (2). Dependence of $\langle D \rangle$ versus t_d for PPO in bulk (5) and in pores of samples N1 (8), N2 (7), N3 (6).

3.2. Estimation of NMR relaxation effect on self-diffusion data

Both EA and NMR relaxation in porous systems are known to be complicated (displaying "multiphase" behaviour) [11]. So EA can be expressed in the form (4). In this case one should estimate the effect of non-exponentiality of relaxation on time dependent echo-attenuation. For this purpose we obtained the echo-attenuations for two values of the initiation period of the pulse sequence. The largest value of initiation period was defined from the condition of recovery of the longitudinal relaxation and was equal 2.5 s. The minimum value was determined by the equipment performance and was equal to 0.2 s. In the latter the amplitude of the signal was half as much as for the first while the shape of the echo-amplitude was the same. The obtained results can be observed only if all protons contributing to the echo-amplitude have the same T_1 or if fast molecule exchange takes place: $\theta_i \ll t_d$, where θ_i is the life time of a proton in the i-th NMR "phase" with $T_1 = T_{1i}$. In both cases the dependence of EA upon the diffusion time in the system is conditioned by the peculiarities of molecular diffusion in the porous medium.

The effect of "multiphase" transverse relaxation was studied by comparing the echo-attenuations derived for different τ_2. The echo-attenuation appeared to be unchanged. Thus, the observed EA variance and the diffusion coefficient dependence upon t_d are caused by the peculiarities of molecular self-diffusion in porous systems.

3.3. Extensions of mean-squared displacement range

The range of diffusion times that are available for measurements is restricted on the side of large t_d values due to the relaxation attenuation of echo intensity (3) and on the side of small t_d due to the technical characteristics of NMR device (the minimum $t_d \sim 1$ ms). Respectively, the accessible molecular displacements are also restricted.

However, the range of displacements may be extended at least in the range of small $\langle x^2 \rangle$, by substituting water by another liquid with a diffusion coefficient smaller than that of water. This liquid should not dissolve gypsum and should be chemically inert with respect to it. An oligomer of polypropyleneoxide (PPO) with the molecular mass of $M = 1025$ was used. The diffusion coefficient of bulk PPO is $1.77 \times 10^{11}\,\mathrm{m^2\,s^{-1}}$ for $T = 30\,^\circ\mathrm{C}$, with the echo-attenuation being close to the exponential value over the 1.5 decimal orders ($\chi \sim 1.04$). The samples N1–N3 were saturated with PPO after completion of water evaporation. Fig. 2 shows $\langle D \rangle$ and χ as functions of diffusion time for PPO in the bulk state and confined in pores of gypsum (samples N1–N3, curves 5–8). It is apparent that the dependence of $\langle D \rangle$ on t_d for PPO essentially differs from that for water in the gypsum. A plateau with $\langle D \rangle \sim 10^{-11}\,\mathrm{m^2\,s^{-1}}$ in the range of $t_d = 100$–10 ms is observed for PPO. For $t_d < 10$ ms $\langle D \rangle$ increases with the reduction of t_d and becomes equal to that of the bulk value when $t_d = 2$ ms is attained. The EA observed in the range of t_d more than 10 ms coincides with that for water in gypsum. Note that when $t_d < 10$ ms the shape of EA changes, the details will be discussed further.

Two curves obtained for different length scales of the liquid molecules displacements in pores of the same samples (curves 2 and 6) could be overlapped if the molecular sizes of both liquids are less than the pore diameter and the effect of pore surface on molecules of both the liquids are equivalent. The size of the water molecule is known. The size of the oligomer molecule can be estimated as the mean-squared distance between the ends of the oligomer chain [12]. This value estimated from the value of statistical segment (0.418 nm [13]) and their molecular mass is equal to 11a. This value and the size of the water molecule are significantly less than the minimum pore dimensions of the hardened gypsum (< 0.05 μm [4]). Interactions between the diffusing molecules and the pore surface are described by the interaction potentials [14] which reduce to zero due to the formation of the adsorbed liquid layers on the pore surface [15]. Because of this we have made an assumption about the equivalence of the interactions of water and PPO molecules with the pore surface. The operation of overlapping was performed by adding a part obtained as a result of conversion of $\langle D\rangle$ and t_d for PPO into $\langle D\rangle$ and t_d proposed for water self-diffusion in pores for the same $\langle x^2\rangle$

$$\begin{aligned} \langle D\rangle_{\text{water}} &= (D_0)_{\text{water}}\langle D\rangle_{\text{PPO}}/(D_0)_{\text{PPO}} \\ t_d &= \langle x^2\rangle/2\langle D\rangle_{\text{water}} \end{aligned} \tag{4}$$

to the experimental dependence observed for water.

The former was written under the above assumption of equivalent effect of porous medium on water and PPO molecules for equal $\langle x^2\rangle$. This allows us to calculate t_d from $\langle x^2\rangle$ and the value of $\langle D\rangle_{\text{water}}$. The dependencies obtained in such a way are presented on Fig. 3. Apparently, the calculated parts overlap with experimental ones. This fact confirms our above assumption. On the whole, the obtained curves characterize the self-diffusion in pores over the length scale estimated according to (1) to be 2.5×10^{-7} m–4.2×10^{-5} m. The parameter of non-exponentiality χ for the samples N1–N3 also are presented in Fig. 3.

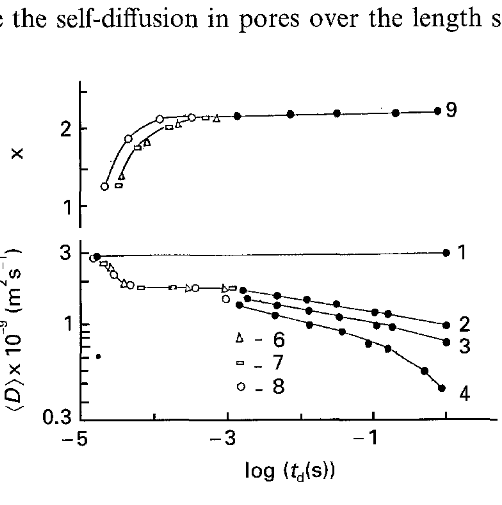

Figure 3 Dependence of $\langle D\rangle$ on t_d for water in bulk (1) and in pores of the samples N1 (4, 8), N2, (3, 7), N3 (2, 6). Curves 2–4 represent the experimental data. Curves 6–8 are computed using the Relation 3. Curve 9 represents the calculated values of χ and obtained experimentally for real diffusion time.

When PPO is injected in samples N4 and N5, the behaviour of the function $\langle D\rangle = f(t_d)$ is similar qualitatively to that for the water contained in samples N1–N3.

3.4. Discussion

One of the observed phenomena is the invariability of EA non-exponential shape in the wide range of diffusion times. Since only liquid molecules contribute to the echo signal, the non-exponentiality of EA is obviously conditioned by their distribution over the states with the different projections of D on a pulsed field gradient vector.

Let us consider the results obtained in terms of molecular self-diffusion in system with molecular exchange between "phases" with different D [16]. In this case the shape of EA depends on the ratios between the value of t_d and the lifetimes τ_1 of the molecules in "phases". For $\tau_i \gg t_d$ the curve EA is non-exponential. When $\tau \ll t_d$ it is exponential. In both cases the shape of EA is independent of t_d. However, if $\tau_i \sim t_d$ the shape of EA is non-exponential and depends upon t_d.

One may try to explain the unchanged EA shape by two factors.

1. The slow exchange between the states with different D ($\tau_i \gg t_d$).
2. The intermediate exchange between the states ($\tau_i \sim t_d$). In the latter case, molecules reach the semipermeable obstacles of greater length scale as t_d increases, thus the exchange effect is equalized.

However, we cannot explain the constant shape of EA by the second factor. Indeed, the more mobile molecules collide with the obstacles with increasing extent then slow during the process of diffusion. This inevitably tends to the exponential EA shape. The first factor also does not fit the experimental data since it cannot explain the dependence of $\langle D\rangle$ upon t_d.

Comparison of both dependencies of $\langle D\rangle$ and χ on t_d (see Fig. 3) shows an existence of correlation between the variations of these parameters in the interval of short t_d, but for the large values of t_d no correlation is observed. While χ remains constant, D is dependent upon t_d. So we assumed that for these values of t_d, both observed effects are due to different causes: the evolution of EA shape reflects the slow molecular exchange between the states with different values of D while the dependence of $\langle D\rangle$ on t_d, most probably, arises from restricted diffusion which is caused by barriers to molecular motions in these states [17]. The non-exponentiality of EA caused by diffusion in the semipermeable system with restrictions is practically negligible with respect to that caused by the existence of a set of states with different D.

A different approach represents the theoretical computation of EA for possible models and the comparison of computed curves with experimental ones. The non-exponentiality of EA at $\langle D\rangle$ independent upon

t_d can be described by a model of low dimensional anisotropic diffusion. The most simple example of a medium providing anisotropic self-diffusion is the system comprised of randomly oriented capillaries or the system of void space having laminated morphology without molecular exchange between structural compartments. The relations describing EA in these models are reported in [18]. We found that the relation obtained for the motion of molecules trapped between flat surfaces of different orientations corresponds to the experimental EA for water in the gypsum pores over the whole range (Fig. 1). This relation is [18]:

$$R(g) = \exp(-kD_0)\int_0^1 \exp(kD_0x^2)\mathrm{d}x \qquad (5)$$

where $x = \cos(\vartheta)$, and ϑ is the angle between a normal to the surface layer and the pulsed gradient vector. The experimental value of $\langle D\rangle$ is not dependent upon t_d and equal to $\langle D\rangle = D_2 = D_0/1.5$. At the temperature 30 °C the value of D_2 for water is $1.8\times10^{-9}\ \mathrm{m^2\,s^{-1}}$. We assumed that the samples of gypsum under consideration have also the layered morphology. Then the observed spectrum of D is conditioned by the random layer orientations with respect to the gradient direction. The largest and the smallest values of D characterize the diffusion in the layers directed parallel and across the pulsed gradient.

The fact that $\langle D\rangle$ does not exceed the value $D_2 = 1.8\times10^{-9}\ \mathrm{m^2\,s^{-1}}$ and is tending to it as t_d reduces in the whole range of t_d when $\chi = 2.2$ (Figs 2 and 3) confirms the above assumption. The layers with different orientations with respect to the pulsed gradient vector comprise the states of molecules with different D, which we have found by considering the first approach.

During crystallization of gypsum the lattice of layered structure is formed [2, 3]. Under conditions close to thermodynamic equilibrium (when water is in excess) the thin layered crystallites are formed [2]. This structure is observed in the pictures of native [2] and of artificially hardened gypsum [3]. In the case of crystallization under conditions far from thermodynamic equilibrium, plates forming the layers are interconnected by numerous crystallites. They serve as the barriers for motion of liquid molecules trapped between the layers. The layered structure is exhibited by the space-time correlation of liquid molecule diffusion. The main elements of such a structure are sketched in Fig. 4.

We can evaluate some of the structural parameters of the model using experimental curves (Figs 2 and 3). The plateau in the region of small t_d values is observed when $\langle D\rangle \sim D_2$ (Fig. 3). In this case the shape of EA remains unchanged and is described by Equation 5. The plateau region represents the translations of molecules within distances less than the barrier spacings. Its existence shows in that the layer width is smaller than the mean separation between the barriers. The subsequent reducing of t_d leads to an increase of $\langle D\rangle$ up to the bulk value D_0. The unrestricted diffusion of molecules between the layers is observed when the mean-squared displacement is equal to the above calculated value of layer width ($\sim 2.5\times10^{-7}$ m). At the condition of slow exchange between the liquid in layers of different directions (for the maximum t_d and corresponding $\langle D\rangle$), the smallest possible value of layer stretching for each sample can be estimated for the largest molecular displacement by Equation 1. These values are equal to 2.8×10^{-5} m (N1), 3.7×10^{-5} m (N2), and 4.2×10^{-5} m (N3).

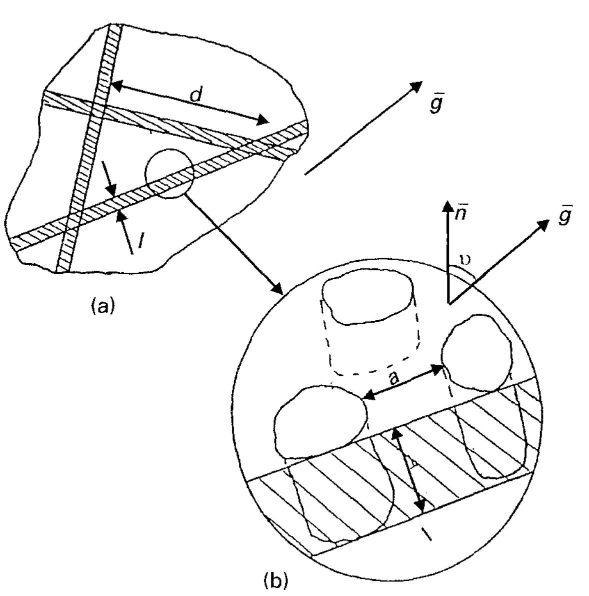

Figure 4 Elements of the probable structure of hardened gypsum derived from the NMR PMFG data: system comprising a random distribution of the planar layers with respect to the gradient direction (a), and the part of the planar layer (b). Here 1 is the layer width, *d* is the spacing between the layers, *n* is the normal to the plane, and *a* is the separation between the barriers. Proportions between the elements were chosen arbitrarily.

The slope of $\langle D\rangle$ versus t_d is defined by liquid molecule collisions with the barriers. The barriers are probably the secondary crystalline structures, formed in the cavities of the primary framework from residual sufficiently saturated solution [3]. Using an extrapolation of the experimental dependence into the range of small t_d up to attaining the value D_2 (Fig. 2) and Equation 1, one can estimate the barrier separations in the layers. The obtained values are 0.6×10^{-6} m (N1), 1.4×10^{-6} m (N2), and 2×10^{-6} m (N3).

Thus, the proposed model does not contradict the known peculiarities of the gypsum structure and is a more detailed one. The dependence of $\langle D\rangle$ upon t_d while EA shape is unaffected by t_d and described by Equation 5, also have been found by Callaghan and co-worker [19] when they studied the water self-diffusion in the lamellar phase of a lipid. They have proposed the model of flat layers oriented in the same way as the lipid domains. The observed dependence of $\langle D\rangle$ upon t_d is caused by molecular diffusion between the domains with different orientations of the layers. Virtually the shape of EA (5) is indicative of some form of low dimensional anisotropic transitions of molecules with respect to the gradient. The transitions of water molecules between the layers of lipid are similar to the exchange between the states with different molecular mobility [16]. The shape of EA tend to the exponential one as t_d increases and $\langle D\rangle$ is independent of t_d. Thus Callaghan's interpretation cannot describe the experimental data.

The present model allows one to explain the self-diffusion of liquid molecules confined in the gypsum pores in the most simple way.

Acknowledgment

The authors thank Professor V. D. Skirda from Kazan State University for the helpful discussions and valuable advice.

References

1. S. J. GREGG and K. W. SING, "Adsorption, Surface Area, and Porosity" (Academic Press, London, 1982).
2. P. P. BUDNIKOV, "Gypsum" (Izd. Akad. Nauk, Leningrad, 1993) (in Russian).
3. I. M. LJASHKEVICH, "Gypsum in Construction Materials" (Vischaja Skola, Minsk, 1989) (in Russian).
4. Der Baustoff Gips, "Stoffliche Grundlagen, Herstellund und Anwendung von Gipsbauelementen", edited by H. Brukner (Veb Verlag fur Bauwesen, Berlin, 1978).
5. D. AVNIR, D. FARIN, D and P. PFEIFER, *Nature* **308** (1984) 261.
6. S. HAVLIN and D. BEN-AVRAHAM, *Adv. Phys.* **36** (1987) 695.
7. J. P. TANNER and E. O. STEJSKAL, *J. Chem. Phys.* **49** (1968) 1768.
8. J. KARGER, H. PFEIFER and W. HEINK, *Adv. Magn. Res.* **12** (1989) 1.
9. P. T. CALLAGHAN, *Aust. J. Phys.* **37** (1984) 359.
10. A. I MAKLAKOV, V. D. SKIRDA and N. F. FATKULLIN, "Encyclopedia of Fluid Mechanics", Vol. 9. Polymer Flow Engineering (Gulf Publ. Co., Houston, 1990).
11. A. I. MAKLAKOV, V. D. SKIRDA and N. F. FATKULLIN, "Self-Diffusion in Polymer Solutions and Melts" (Izd. Kazan. Univ., Kazan, 1987) (in Russian).
12. P. J. FLORY, "Statistical Mechanics of Chain Molecules" (Interscience Publishers, New York, 1969).
13. V.P. PRIVALKO, "Structure and Properties of Polymer" (Naukova Dumka, Kiev, 1984) (in Russian).
14. N. F. FATKULLIN, *Zh. Eksp. Teor. Fiz.* **98** (1990) 2030 [*Sov. Phys. JETP* **71** (1990) 1141].
15. N. F. FATKULLIN, private communication (1994).
16. J. KARGER, *Ann. Phys.* **24** (1969) 1.
17. A. V. FILIPPOV, E. V. KHOSINA and V. G. KHOSIN, *Khimicheska ja Fizika* **12** (1993) 1519.
18. P. T. CALLAGHAN, K. W. JOLLEY and J. LELIEVRE, *Biophys. J.* **28** (1979) 133.
19. P. T. CALLAGHAN and O. P. SODERMAN, *J. Phys. Chem.* **87** (1983) 1737.

Received 4 July 1994
and accepted 19 September 1995